Targeting BCL2 with Venetoclax Enhances the Efficacy of the *KRAS*^{G12D} Inhibitor MRTX1133 in Pancreatic Cancer

Jeffrey H. Becker[1,2], Anastasia E. Metropulos[1,2], Christina Spaulding[1,2], Alejandra M. Marinelarena[1], Mario A. Shields[1,3], Daniel R. Principe[1], Thao D. Pham[1,3], and Hidayatullah G. Munshi[1,2,3]

ABSTRACT

MRTX1133 is currently being evaluated in patients with pancreatic ductal adenocarcinoma (PDAC) tumors harboring a *KRAS*^{G12D} mutation. Combination strategies have the potential to enhance the efficacy of MRTX1133 to further promote cell death and tumor regression. In this study, we demonstrated that MRTX1133 increased the levels of the proapoptotic protein BIM in PDAC cells and conferred sensitivity to the FDA-approved BCL2 inhibitor venetoclax. Combined treatment with MRTX1133 and venetoclax resulted in cell death and growth suppression in 3D cultures. BIM was required for apoptosis induced by the combination treatment. Consistently, BIM was induced in tumors treated with MRTX1133, and venetoclax enhanced the efficacy of MRTX1133 *in vivo*. Venetoclax could also resensitize MRTX1133-resistant PDAC cells to MRTX1133 in 3D cultures, and tumors established from resistant cells responded to the combination of MRTX1133 and venetoclax. These results provide a rationale for the clinical testing of MRTX1133 and venetoclax in patients with PDAC.

Significance: The combination of MRTX1133 and the FDA-approved drug venetoclax promotes cancer cell death and tumor regression in pancreatic ductal adenocarcinoma, providing rationale for testing venetoclax with *KRAS*^{G12D} inhibitors in patients with pancreatic cancer.

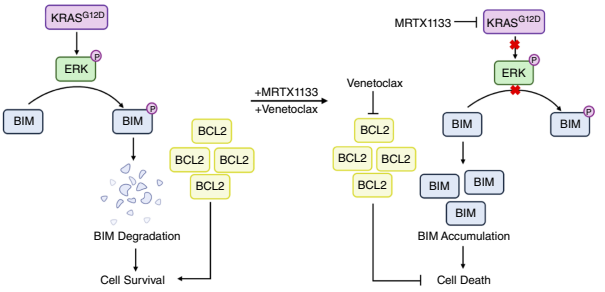

Introduction

Pancreatic ductal adenocarcinoma (PDAC) is currently the third leading cause of cancer-related death in the United States. Despite advances in surgery, radiation, chemotherapy, and immunotherapy, the 5-year survival rate for patients with PDAC is ~13% (1–3). Mutational activation of the *KRAS* gene, critical for PDAC initiation and maintenance in mouse models (4, 5), is present in more than 90% of human PDAC tumors, with *KRAS*^{G12D} mutation accounting for ~45% of the KRAS mutants (6, 7). Recently, inhibitors targeting *KRAS*^{G12C}, present in ~1% to 2% of human PDAC tumors, have been developed and tested in patients with PDAC (8, 9). However, single-agent treatment with *KRAS*^{G12C} inhibitors mainly demonstrates brief disease stabilization, with cancer cells activating bypass pathways and developing resistance to KRAS inhibitors (8, 9). As inhibitors of the more common *KRAS* mutations in PDAC are now emerging and with the *KRAS*^{G12D} inhibitor MRTX1133 in the early phase of clinical testing (10), there is increasing interest in identifying novel combination strategies to further enhance the efficacy of KRAS inhibitors (11, 12).

Several combination therapies with MRTX1133 have been tested in preclinical models. For example, in xenograft mouse studies, the efficacy of MRTX1133 in human tumors is enhanced by combining it with an EGFR antibody (13). In immunocompetent mice, as the T cells contribute to the effects of MRTX1133 in PDAC models (14, 15), the efficacy can be enhanced by combining with immune checkpoint inhibitors (15). Notably, although MRTX1133 effectively suppresses cancer cell proliferation in tumors in immunocompetent mice, $CD8^+$ T cells are required to induce cell death and tumor regression (15). The finding that MRTX1133 primarily suppresses cancer cell proliferation without directly inducing apoptosis in immunocompetent mouse model suggests a need to identify additional combination regimens with *KRAS*^{G12D} inhibitors that promote cell death and tumor regression.

The intrinsic (mitochondrial) apoptosis pathway is tightly regulated by the BCL2 protein family, which includes the BH3-only proapoptotic proteins (e.g., BIM), the multidomain effector proteins BAK and BAX, and the antiapoptotic proteins (e.g., BCL2; refs. 16–18). The BCL2 family of antiapoptotic proteins restrains cell death mediators to maintain cellular viability (16–18). In contrast, the BH3-only proapoptotic proteins inhibit the pro-survival BCL2 proteins to induce apoptosis (16–18). Significantly, these proteins can be regulated through posttranslational mechanisms. For example, ERK1/2 signaling can promote phosphorylation and subsequent proteasome-dependent degradation of BIM (19–21).

[1]Department of Medicine, Feinberg School of Medicine, Northwestern University, Chicago, Illinois. [2]Jesse Brown VA Medical Center, Chicago, Illinois. [3]The Robert H. Lurie Comprehensive Cancer Center, Chicago, Illinois.

J.H. Becker and A.E. Metropulos contributed equally to this article.

Corresponding Author: Hidayatullah G. Munshi, Department of Medicine, Feinberg School of Medicine, Northwestern University, 303 East Superior Avenue, Lurie 3-117, Chicago, IL 60611. E-mail: h-munshi@northwestern.edu

Cancer Res 2024;84:3629–39

doi: 10.1158/0008-5472.CAN-23-3574

In this study, we demonstrate that although MRTX1133 increases BIM protein levels, MRTX1133 fails to suppress the growth or induce apoptosis of tumor cells grown in confluent 3D collagen cultures. However, adding the FDA-approved BCL2 inhibitor venetoclax to MRTX1133 induces cell death and suppresses growth in confluent 3D collagen cultures. We also show that BIM is induced in tumors treated with MRTX1133 and demonstrate that venetoclax enhances the efficacy of MRTX1133 *in vivo*. We have also found that venetoclax can resensitize the resistant cells to MRTX1133 in collagen cultures, and tumors established from the resistant cells respond to the combination of MRTX1133 and venetoclax. These results provide a rationale for the clinical testing of MRTX1133 and venetoclax in patients with PDAC.

Materials and Methods

Chemicals

MRTX1133 (HY-134813), trametinib (HY-10999), and venetoclax (HY-1553) were purchased from MedChemExpress. zVAD-FMK (S7073) and additional venetoclax (S8048) were purchased from Selleck Chemicals. The membrane-permeable thiazolyl blue tetrazolium bromide (MTT) dye (ab146345) and the thymidine analog 5-bromo-2′-deoxyuridine (BrdU; ab142567) were obtained from Abcam.

Tumor cell lines

Mouse PDAC cell lines KPC-2138 (2138) and KPC-3213 (3213) were derived from PDAC tumors developing in the KPC (*LSL-Kras*$^{G12D/+}$*/LSL-Trp53*$^{R172H/+}$*/Pdx-1-Cre*) mouse model in the C57BL/6 background (22). KPC-1245 (1245) cell line was provided by David Tuveson (Cold Spring Harbor Laboratory; ref. 23). KPC-K cell lines were generated by culturing KPC cells over 6 weeks in increasing concentrations of MRTX1133 to ≥2 μmol/L, with cells maintained in 2 μmol/L MRTX1133. The human PDAC cell line PANC1 was obtained from ATCC (CRL-1469). PANC1-K cells were generated similarly to the KPC-K cell lines and maintained in 2 μmol/L MRTX1133. The mouse and human PDAC-K cell lines were cryopreserved after being generated. All cell lines were used within 15 passages after revival from frozen stocks. These cell lines did not undergo authentication and were not tested for *Mycoplasma*. All cell lines were cultured in DMEM supplemented with 10% FBS and antibiotics (100 U/mL penicillin and 100 μg/mL streptomycin).

Floating collagen gel cultures

Acidified rat tail collagen I (Corning) was neutralized with 0.34 N NaOH and diluted to a final concentration of 1.2 mg/mL (24). Single-cell suspensions were mixed with diluted collagen to obtain 10^5 cells/mL, and 1 mL of collagen/cell mixture was plated into ultra-low attachment six-well plates (Corning; refs. 25, 26). After 1 hour of polymerization at 37°C, 2 mL of the media was added, and the gels were detached from the well using a fine pipette tip. For "low"-confluent collagen cultures, the cells in the floating collagen gels were treated after 48 hours, whereas for the "high"-confluent collagen cultures, the cells were treated after 96 to 120 hours. The cells were imaged using the EVOS XL Core Imaging System (Thermo Fisher Scientific), and the relative growth was quantified.

BIM knockdown

Silence-select predesigned siRNA against mouse Bim (s201095) and human BIM (195011) were obtained from Thermo Fisher Scientific. The siRNA transfections were carried out using RNAiMAX (Invitrogen) according to the manufacturer's instructions (27).

MTT assay

PDAC cells were seeded in low density (2×10^3 cells/well) or high density (10×10^3 cells/well) in each well of a 96-well plate in serum-free DMEM. After 16 hours, media and drugs were added, and cells were cultured for 72 hours. At this time, 20 μL of a 5 mg/mL MTT solution was added to each well (1:10). After 2 hours, media was aspirated, crystals were dissolved in DMSO, and 570-nm absorbance was determined by a plate reader (28).

BrdU incorporation assay

PDAC cells growing in "low"- and "high"-confluent 3D collagen cultures were treated with 2 μmol/L BrdU for 1 hour. Cells were extracted from collagen gels using collagenase I (Worthington Biochemical), fixed with 4% paraformaldehyde, and then collected for immunocytochemistry. Antigen retrieval was carried out at 37°C in 2 N HCl for 1 hour. The slides were incubated with 1% BSA/PBS for 1 hour at room temperature. The cells were stained overnight at 4°C with BrdU antibody (MoBU-1, B35139, Thermo Fisher Scientific, RRID:AB_2536439) at 1:100 dilution followed by secondary Alexa Fluor 488 antibody (A32723, Thermo Fisher Scientific, RRID:AB_2633275). The nuclei were costained with DAPI, and the slides were mounted and visualized using the EVOS M7000 microscope (Thermo Fisher Scientific) and quantified using ImageJ.

Western blot analysis

Cells were extracted from collagen gels using collagenase I (Worthington Biochemical) and lysed in RIPA buffer supplemented with phosphatase and protease inhibitors (Calbiochem; ref. 29). Equal amounts of protein were run in reducing conditions as described previously (22, 29). The following antibodies were used at the dilution recommended by the manufacturers: pERK1/2 (#9101, Cell Signaling Technology, RRID:AB_331646), total ERK1/2 (#9102, Cell Signaling Technology, RRID:AB_330744), mouse BIM (#2933, Cell Signaling Technology, RRID:AB_1030947), mouse BCL2 (554218, BD Pharmingen, RRID:AB_395311), cleaved caspase-3 (c-C3; #9664, Cell Signaling Technology, RRID:AB_2070042), human BCL2 (#3498, Cell Signaling Technology, RRID: AB_1903907), PARP (#9542, Cell Signaling Technology, RRID:AB_2160739), HSP90 (#4877, Cell Signaling Technology, RRID:AB_2233307), and GAPDH (MAB374, MilliporeSigma, RRID:AB_2107445). Secondary anti–mouse IgG were purchased from Sigma-Aldrich (A4416, RRID:AB_258167) or Cell Signaling Technology (#7076, RRID: AB_330924). Anti–rabbit IgG antibodies were purchased from Sigma-Aldrich (A6667, RRID:AB_258307) or Cell Signaling Technology (#7074, RRID:AB_2099233).

Animal studies

For subcutaneous tumor studies, 2138, 3213, 1245, 2138-K, 3213-K, and 1245-K cells (25×10^3 cells/100 μL of Matrigel) were injected under the skin into the flanks of 6- to 8-week-old C57BL/6 mice. When tumors achieved a volume of ~250 to 300 mm^3 for 2138, 3213, and 1245 cells or ~80 to 100 mm^3 for 2138-K, 3213-K, and 1245-K cells, mice were randomized and treated with vehicle control, MRTX1133 (30 mg/kg 2× daily; refs. 13–15), venetoclax (15 mg/kg daily; ref. 30), or the combination of MRTX1133 and venetoclax. In additional experiments, 2138,

3213, and 1245 tumors measuring ~80 to 100 mm^3 were treated with vehicle control or MRTX1133 (30 mg/kg 2× daily). Tumor volume was calculated using the formula $V = (W^2 \times L)/2$, in which V is the tumor volume, W is the tumor width, and L is the tumor length by caliper measurement. At the study endpoint (e.g., tumor volume exceeding 1,200–1,500 mm^3, tumor ulceration, weight loss of >20%, or weakness and inactivity), tumor-bearing mice were euthanized by CO_2 inhalation and cervical dislocation.

IHC staining and analysis

Mouse tumors were stained for pERK (#9101, Cell Signaling Technology, RRID:AB_331646, 1:100), Bim (#2933, Cell Signaling Technology, RRID:AB_1030947, 1:1,200), and c-C3 (#9664, 1:1,000, Cell Signaling Technology, RRID:AB_2070042). Antigen retrieval was carried out, as previously described (31), with either pH 6.0 or pH 9.0 buffer according to the manufacturer's instructions. After antigen retrieval, tumor sections were incubated with BLOXALL (VectorLabs) for 20 minutes at room temperature. Sections were incubated with primary antibodies in 1% BSA/PBS overnight at 4°C. ImmPRESS Secondary HRP anti–rabbit IgG (Peroxidase) Polymer Detection Kit was purchased from VectorLabs. Photographs were taken on the FeinOptic microscope using the Jenoptik ProgRes C5 camera, and pERK, BIM, and c-C3 signals were quantified. At least five different fields of view were examined for final quantification.

Immunofluorescence staining

For tumor specimens, antigen retrieval was carried out as previously described using pH 6.0 citrate buffer (28). After antigen retrieval, sections were incubated with 10% normal goat serum (Agilent) for 20 minutes at room temperature, followed by incubation with 1% BSA/PBS buffer for 1 hour at room temperature. The sections were incubated with Ki67 (#12202, 1:1,000, Cell Signaling Technology, RRID:AB_2620142) and cytokeratin 19 (CK19, 1:100, DHSB, RRID:AB_2133570) in 1% BSA/PBS overnight at 4°C. Secondary Alexa Fluor 488 and Alexa 647 antibodies were purchased from Thermo Fisher Scientific and used at 1:400 to 1:1,000 dilution factor. DAPI was used to counterstain the nuclei. Final pictures, taken on the EVOS M7000 microscope, were quantified using ImageJ. At least five different fields of view were examined for final quantification.

Statistical analysis

Error bars represent the SEM or SD, as specified in the figure legends. The values for n, P, and the specific statistical test performed for each experiment are specified in the figure legends. All statistical analyses were done using GraphPad. A $P < 0.05$ value was considered significant.

Study approval

All animal work and procedures were approved by the Northwestern University Institutional Animal Care and Use Committee. The animal experiments were performed in accordance with relevant guidelines and regulations.

Data availability

All raw data generated in this study are available upon request from the corresponding author.

Results

MRTX1133 inhibits the growth of PDAC cells in "low"- but not "high"-confluent collagen cultures

PDAC is hallmarked by a desmoplastic collagen-rich stroma that is not represented in traditional 2D cell culture systems (32, 33). As cells grown in 3D floating collagen gels better mirror tumor morphogenesis than those grown on plastic (25, 26), we utilized the floating collagen gel system to test the efficacy of MRTX1133 against PDAC cell lines. When tested in "low"-confluent collagen cultures (**Fig. 1A**), MRTX1133 suppressed ERK1/2 phosphorylation and effectively blocked the growth of mouse and human PDAC cell lines (**Fig. 1B** and **C**). However, when tested in "high"-confluent collagen cultures (**Fig. 1D**), MRTX1133, even though it blocked ERK1/2 phosphorylation (**Fig. 1E**), failed to suppress the growth of these cell lines (**Fig. 1F**).

To understand the differential response to MRTX1133 in "low"- and "high"-confluent collagen cultures, we evaluated the effect of confluency on PDAC cell proliferation. PDAC cells in "low"- and "high"-confluent collagen cultures were treated with MRTX1133 for 8 hours, and BrdU was added an hour before collection. The samples were processed for BrdU incorporation by immunocytochemistry. Cells in "high"-confluent collagen cultures exhibit reduced BrdU incorporation compared with cells in "low"-confluent collagen cultures, indicating that the cells in "high"-confluent cultures proliferate significantly slower (Supplementary Fig. S1). Although MRTX1133 decreases BrdU incorporation in both "low"- and "high"-confluent collagen cultures, the effect was more pronounced in the "low"-confluent collagen cultures (Supplementary Fig. S1).

PDAC cells grown on tissue culture plastic exhibit increased sensitivity to MRTX1133 in "low"- confluent than in "high"-confluent 2D cultures

Given the lack of efficacy of MRTX1133 in "high"-confluent collagen cultures, we evaluated the efficacy of MRTX1133 in PDAC cells plated in "low" and "high" density on tissue culture plastic. We show that although MRTX1133 suppresses ERK1/2 phosphorylation in both "low"- and "high"-confluent 2D cultures (Supplementary Fig. S2A and S2B), MRTX1133 has minimal effect on suppressing the cell viability in "high"-confluent 2D cultures (Supplementary Fig. S2C). Moreover, consistent with a recent report (34), the efficacy of MRTX1133 in "low"-confluent cultures is lower when cells are grown on 2D tissue culture plastic compared with when cells are grown in 3D collagen gels (Supplementary Figs. S1C and S2C).

MRTX1133 increases the levels of the proapoptotic protein BIM

The KRAS/MEK/ERK pathway is a central regulator of cell survival and can suppress apoptosis (5, 35). For example, the MEK/ERK signaling can decrease the protein levels of the proapoptotic BIM by promoting its degradation (19–21). Thus, to identify potential combination strategies to improve the efficacy of MRTX1133 in "high"-confluent 3D collagen cultures, we evaluated the effects of MRTX1133 on the proapoptotic BIM. We found that MRTX1133, like the MEK inhibitor trametinib, increased the levels of the BIM protein in PDAC cells (**Fig. 2A**).

Venetoclax enhances the efficacy of MRTX1133 in "high"-confluent collagen cultures

Despite the increase in BIM protein levels, MRTX1133 failed to suppress the growth of tumor cells in "high"-confluent collagen cultures. Thus, to alter the balance between pro- and antiapoptotic

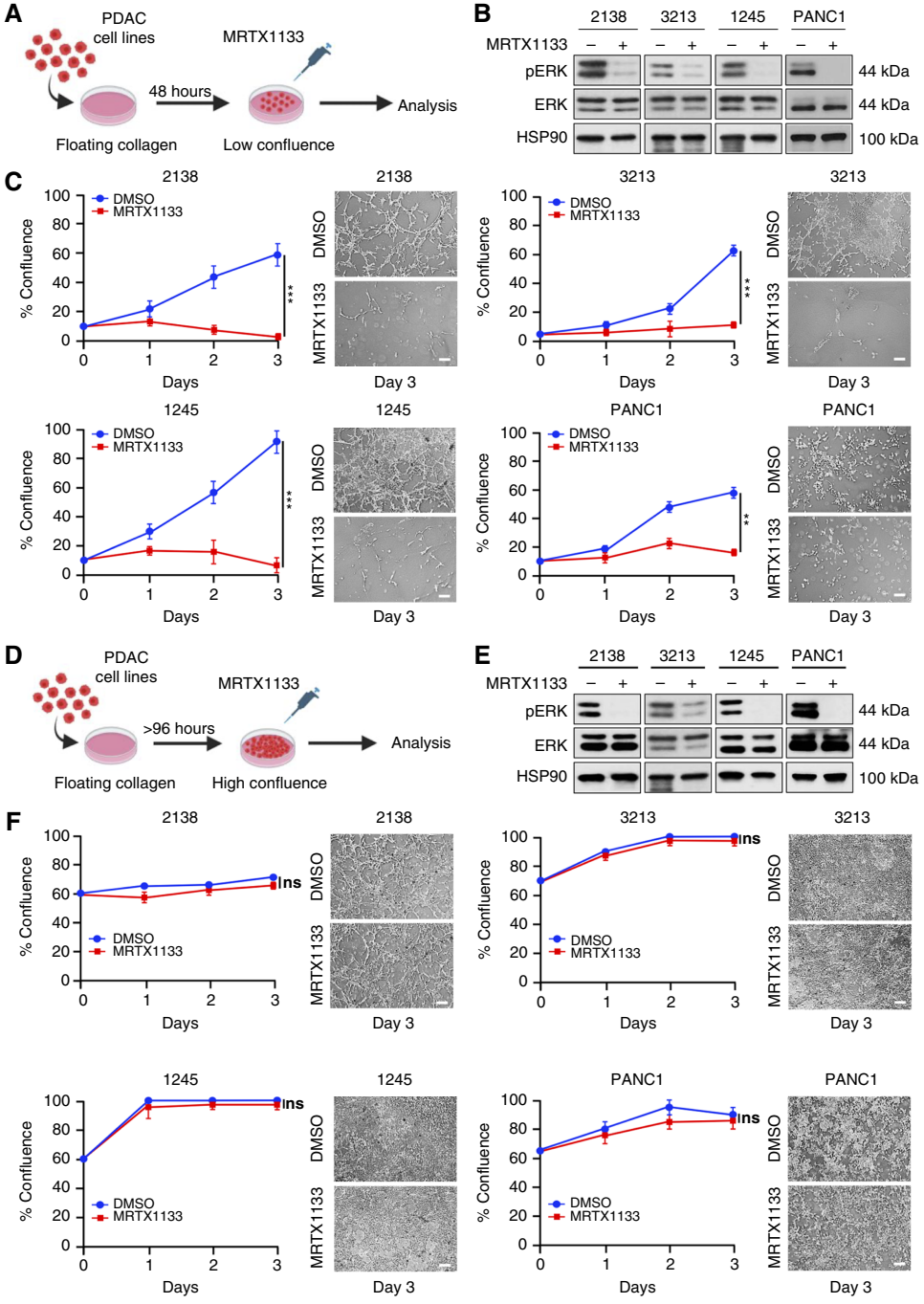

Figure 1.

MRTX1133 inhibits the growth of PDAC cells in "low"- but not "high"-confluent collagen cultures. **A,** PDAC cells (1×10^5) were grown in floating collagen gels (1.2 mg/mL) for 48 hours to generate "low"-confluent cultures. Depiction of "low"-confluent floating collagen cultures. **B,** PDAC cell lines (2138, 3213, 1245, PANC1) grown in "low"-confluent collagen cultures were treated with MRTX1133 (0.5 μmol/L) for 8 hours, and the effect on ERK1/2 phosphorylation was analyzed by Western blotting. Blots are representative of at least three biological replicates. **C,** PDAC cell lines grown in "low"-confluent collagen cultures were treated with DMSO or 0.5 μmol/L MRTX1133 for 72 hours. The cells were imaged at baseline and after 1, 2, and 3 days of treatment, and the relative growth was quantified. Error bars, ± SD; $n = 3$, unpaired t test. **, $P < 0.01$; ***, $P < 0.001$. Scale bar, 100 μm. **D,** PDAC cells (1×10^5) were grown in floating collagen gels (1.2 mg/mL) for 96 to 120 hours to generate "high-confluent" cultures. Depiction of "high-confluent" floating collagen cultures. **E,** PDAC cell lines grown in "high-confluent" collagen cultures were treated with MRTX1133 (0.5 μmol/L) for 8 hours, and the effect on ERK1/2 phosphorylation was analyzed by Western blotting. Blots are representative of at least three biological replicates. **F,** PDAC cell lines grown in "high-confluent" collagen cultures were treated with DMSO or 0.5 μmol/L MRTX1133 for 72 hours. The cells were imaged at baseline and after 1, 2, and 3 days of treatment, and the relative growth was quantified. Error bars, ± SD; $n = 3$, unpaired t test. ns, not significant. Scale bar, 100 μm.

proteins toward apoptosis, we treated the cells with the FDA-approved BCL2 inhibitor venetoclax (36, 37). MRTX1133 had minimal to no effects on the antiapoptotic protein BCL2 in PDAC cells (**Fig. 2A**). Although venetoclax did not induce apoptosis (c-C3 or cleaved-PARP) or suppress the growth of collagen cultures (**Fig. 2B** and **C**), adding venetoclax to MRTX1133 significantly induced cell death and suppressed growth of "high"-confluent 3D collagen cultures (**Fig. 2B** and **C**).

We also evaluated the combination of venetoclax and MRTX1133 in PDAC cells grown on 2D tissue culture plastic. In contrast to the effect of venetoclax in 3D collagen culture, venetoclax had minimal to no effect on the ability of MRTX1133 to decrease the cell viability of PDAC cells grown on 2D tissue culture plastic (Supplementary Fig. S3).

BIM is required for apoptosis induced by the combination therapy in "high"-confluent collagen cultures

As we found that the induction of BIM was not sufficient for MRTX1133 to induce cell death, we evaluated whether BIM was required for the response of the combination treatment with MRTX1133 and venetoclax in cells grown in "high"-confluent 3D

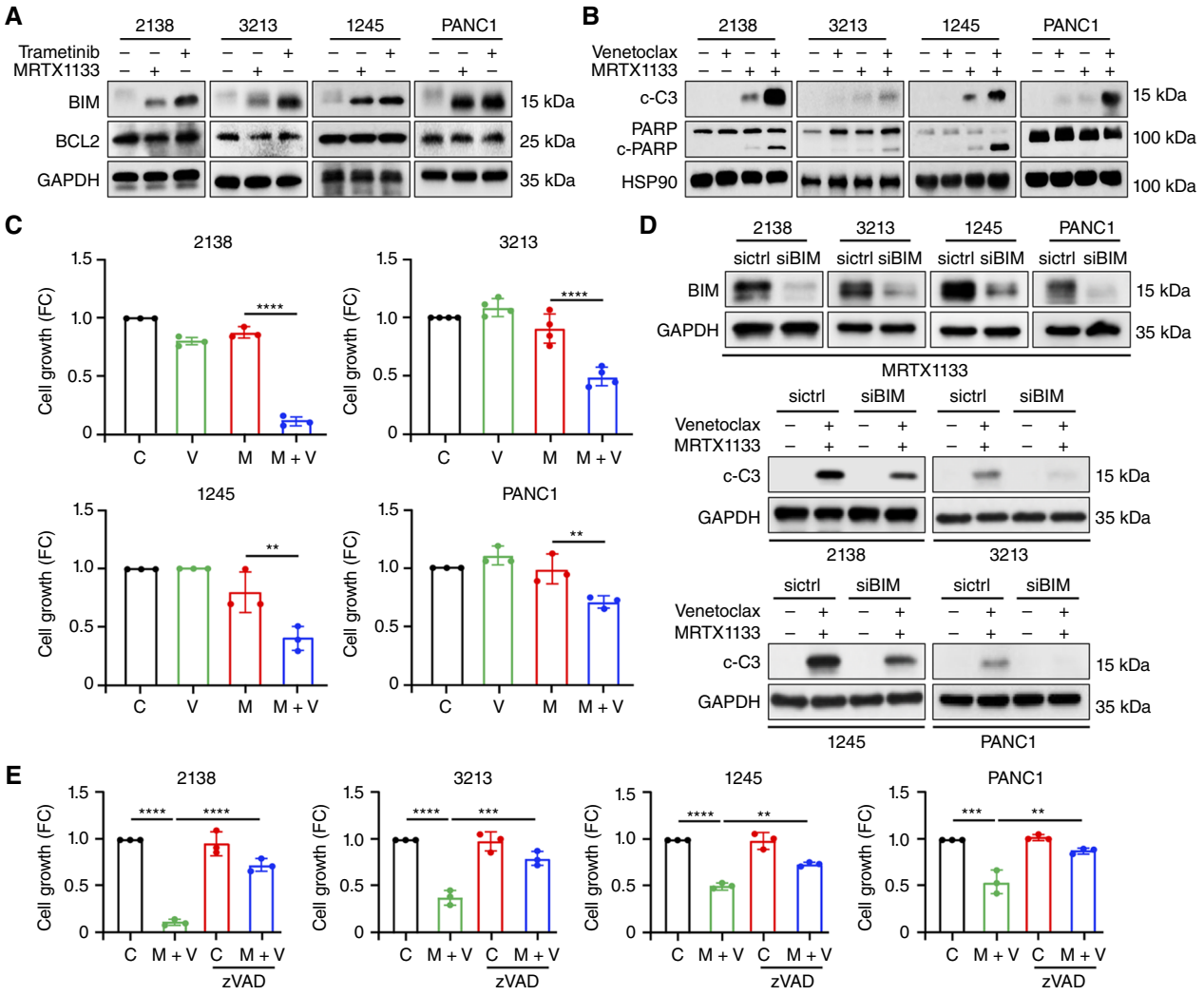

Figure 2.

BCL2 inhibitor venetoclax enhances the efficacy of MRTX1133 in "high"-confluent collagen cultures. **A,** PDAC cells (2138, 3213, 1245, and PANC1) in "high"-confluent collagen cultures were treated with MRTX1133 (0.5 μmol/L) or the MEK1/2 inhibitor trametinib (0.1 μmol/L) for 8 hours. The effect on BIM and BCL2 was analyzed by Western blotting. Blots are representative of at least three biological replicates. **B,** PDAC cells in "high"-confluent collagen cultures were cotreated with venetoclax (2.5 μmol/L) and MRTX1133 (0.5 μmol/L) for 8 hours, and the effect on cell death (c-C3, cleaved-PARP) was analyzed. Blots are representative of at least three biological replicates. **C,** "High"-confluent collagen cultures of PDAC cells were cotreated with venetoclax (V; 2.5 μmol/L) and MRTX1133 (M; 0.5 μmol/L) for 48 hours, and the effect on cell growth was analyzed. Error bars, ± SD; $n = 3$ to 4. One-way ANOVA, followed by the Tukey multiple comparison test. **D,** PDAC cells were transfected with control siRNA or siRNA against BIM for 72 hours, plated in collagen, and treated with MRTX1133 (0.5 μmol/L) for 8 hours. The effect on BIM was analyzed using Western blotting. The transfected cells were also cotreated with venetoclax (2.5 μmol/L) and MRTX1133 (0.5 μmol/L) for 8 hours, and the effect on cell death (c-C3) was analyzed. Blots are representative of three biological replicates. **E,** "High"-confluent collagen cultures of PDAC cells were cotreated with venetoclax (2.5 μmol/L) and MRTX1133 (0.5 μmol/L) for 48 hours with or without the pan-caspase inhibitor zVAD-FMK (zVAD; 10 μmol/L), and the effect on cell growth was analyzed. Error bars, ± SD, $n = 3$. One-way ANOVA, followed by the Tukey multiple comparison test. **, $P < 0.01$; ***, $P < 0.001$; ****, $P < 0.0001$.

collagen cultures. Using siRNA to suppress MRTX1133-induced BIM expression, we show that siRNA against BIM attenuates apoptosis induced by the combination treatment (**Fig. 2D**). We also show that the pan-caspase inhibitor zVAD-FMK limits the growth suppression seen with the combination treatment (**Fig. 2E**).

Venetoclax enhances the efficacy of MRTX1133 *in vivo*

We next evaluated the combination of venetoclax and MRTX1133 *in vivo*. KPC cell lines 2138, 3213, and 1245 were implanted into the flank of syngeneic C57BL/6 mice. Once the tumors reached ~250 to 300 mm^3, the mice were randomized to four treatment groups. Mice received intraperitoneal (IP) injections of DMSO (vehicle control), MRTX1133 (30 mg/kg 2×/day), venetoclax (15 mg/kg daily), or the combination of MRTX1133 and venetoclax. As with our findings in the collagen gels, single-agent treatment with venetoclax did not affect the growth of 2138, 3213, or 1245 tumors (**Fig. 3A**). MRTX1133 had varying effects on the growth of these three KPC cell lines. MRTX1133 prevented the

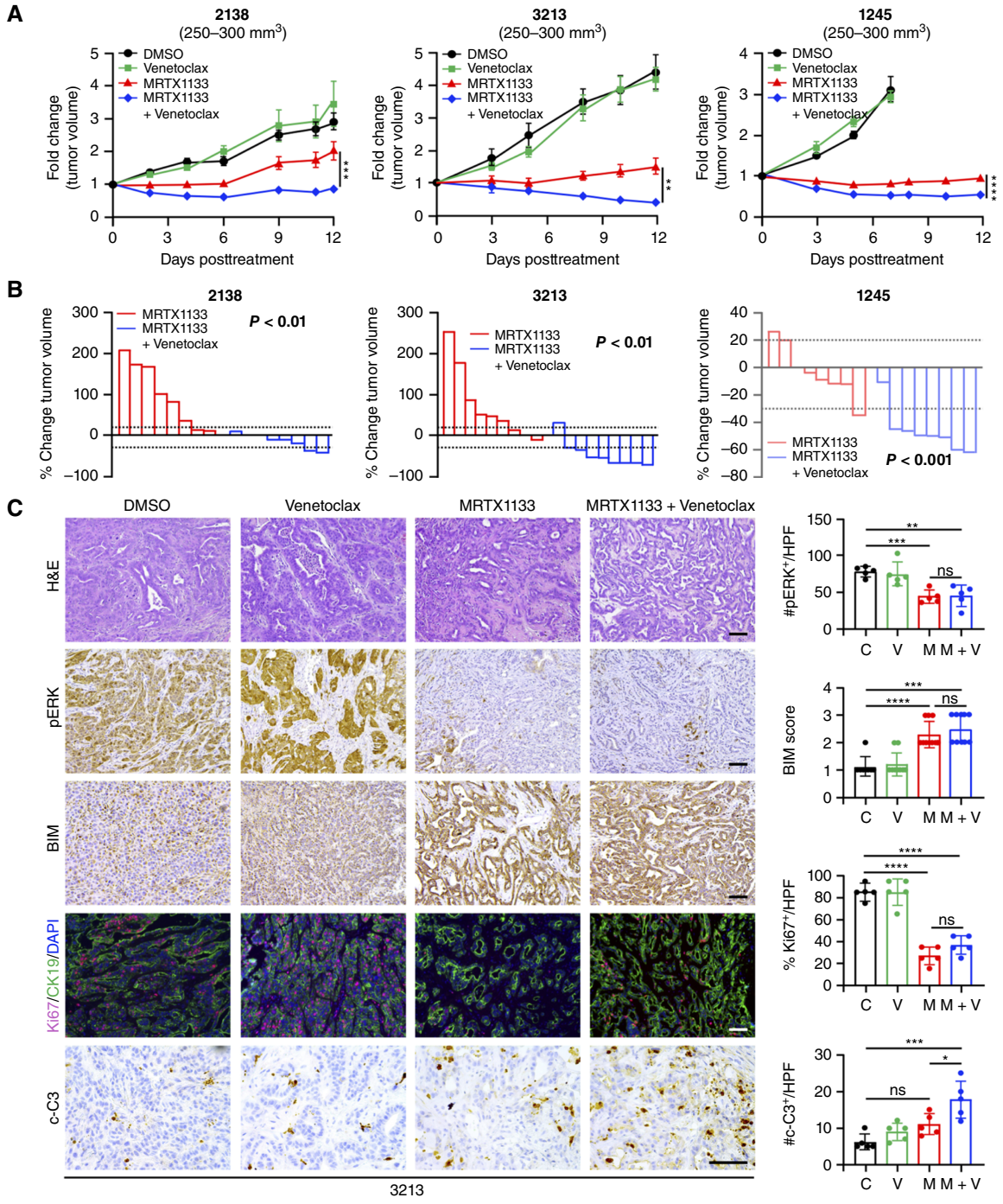

Figure 3.

Venetoclax enhances the efficacy of MRTX1133 *in vivo*. The 2138, 3213, and 1245 KPC cells (2.5×10^4) were implanted via subcutaneous injection into the flanks of C57BL/6 mice. Once animals developed 250 to 300 mm^3 tumors, they were treated with vehicle control (DMSO), venetoclax (15 mg/kg daily), MRTX1133 (30 mg/kg 2×/day), or the combination of venetoclax and MRTX1133. **A,** Tumor size was measured 2 to 3 times/week by caliper, and tumor volume was calculated using the formula $V = (W^2 \times L)/2$ and normalized to tumor volume at the start of treatment. Error bars, ± SEM, $n = 8$ to 9 per treatment group. Significance between the MRTX1133-treated group and the combination treatment group was determined by two-way ANOVA with the Sidak multiple comparisons test. Changes in tumor volume between the dotted lines (−30%, +20%) were considered as stable disease. **B,** Relative tumor volumes at study endpoints were compared with tumors at the start of treatment, and change in tumor volume was calculated. Unpaired *t* test. **C,** 3213 tumors at the study endpoints were hematoxylin and eosin (H&E)–stained and stained for pERK, BIM, the proliferation marker Ki67, the epithelial marker CK19, and the apoptosis marker c-C3. Error bars, ± SD. One-way ANOVA, followed by the Tukey multiple comparison test. *, $P < 0.05$; **, $P < 0.01$; ***, $P < 0.001$; ****, $P < 0.0001$; ns, not significant. Scale bars, 100 μm. C, DMSO; V, venetoclax; M, MRTX1133.

growth of 2138 tumors transiently (**Fig. 3A**). Comparing the tumor volumes at the study endpoint, the majority of the 2138 tumors treated with MRTX1133 showed an increase in tumor size compared with the start of treatment (**Fig. 3B**). Although the 3213 tumors are overall more responsive to MRTX1133 compared with the 2138 tumors, the 3213 tumors showed a similar trend in tumor growth following MRTX1133 treatment as the 2138 tumors (**Fig. 3A** and **B**). In contrast, the single-agent treatment of 1245 tumors with MRTX1133 led to prolonged disease stability (**Fig. 3A** and **B**).

Venetoclax enhanced the efficacy of MRTX1133 in all three KPC tumors. The combination of MRTX1133 and venetoclax suppressed the growth rate of 2138 tumors, resulting in prolonged disease stability (**Fig. 3A** and **B**). In contrast, compared with single-agent treatment with MRTX1133, the combination treatment of 3213 tumors resulted in tumor regression (**Fig. 3A** and **B**). The cotreatment of 1245 tumors with venetoclax and MRTX1133 also resulted in tumor regression (**Fig. 3A** and **B**). Importantly, tumor-bearing mice treated with the combination treatment maintained their body weights (Supplementary Fig. S4), suggesting that the combination treatment was well tolerated.

Histologic analysis of the KPC tumors at the study endpoint showed that MRTX1133 decreased ERK1/2 phosphorylation and induced BIM expression (Supplementary Figs. S3C and S5). Although treatment with MRTX1133, either as a single-agent or as part of the combination treatment, decreased Ki67 staining, only the combination treatment significantly increased staining for c-C3 (Supplementary Figs. S3C and S5).

Venetoclax resensitizes the resistant cells to MRTX1133 in collagen cultures

In additional studies, we established an *in vitro* model of MRTX1133 resistance by culturing PDAC (KPC, PANC1) cell lines over 6 weeks in increasing concentrations of MRTX1133 to ≥2 μmol/L to generate PDAC-K (KPC-K, PANC1-K) cell lines. These mouse and human PDAC-K cell lines are poorly responsive to MRTX1133-induced suppression of ERK1/2 activation in 2D cultures and growth inhibition in 3D collagen cultures (**Fig. 4A** and **B**). Next, we evaluated whether PDAC-K cells upregulated BIM expression when treated with MRTX1133 in collagen cultures. MRTX1133 treatment decreased pERK signaling and upregulates BIM expression in 3D collagen cultures (**Fig. 4C**). Given the BIM upregulation in collagen cultures, we treated the PDAC-K cells growing in collagen cultures with venetoclax. Cotreatment with venetoclax and MRTX1133 resulted in increased apoptosis (c-C3 and cleaved-PARP) and growth suppression in collagen cultures (**Fig. 4D** and **E**).

Tumors established from KPC-K cells respond to the combination of MRTX1133 and venetoclax

Finally, we evaluated the efficacy of the combination of MRTX1133 and venetoclax in tumors established from 2138-K, 3213-K, and 1245-K cells. Due to the rapid growth of some of the KPC-K cells *in vivo* (Supplementary Fig. S6), we treated mice bearing small (~80–100 mm^3) KPC-K tumors (**Fig. 5A**). As with the parental KPC tumors, single-agent treatment with venetoclax did not affect their growth. Although single-agent treatment of 2138-K tumors with MRTX1133 did not slow their growth, single-agent treatment with MRTX1133 of the small 3213-K and 1245-K tumors resulted in disease stability (**Fig. 5A**). To demonstrate that the KPC-K tumors, in particular, the 3213-K and 1245-K tumors, exhibit relative resistance to MRTX1133, we also treated similarly sized (~80–100 mm^3) tumors established from 2138, 3213, and 1245 cell lines with MRTX1133. In contrast to the small 3213-K and 1245-K tumors, the corresponding small parental KPC tumors treated with MRTX1133 demonstrated tumor regression (Supplementary Fig. S7), indicating that the tumors established from the KPC-K cell lines exhibit relative resistance to MRTX1133 *in vivo*.

As with the parental tumors, venetoclax enhanced the response of MRTX1133 in all three KPC-K tumors (**Fig. 5A** and **B**), with mice maintaining their weights with the combination treatment (Supplementary Fig. S8). Although the 2138-K tumors continued to grow, the combination treatment significantly slowed their growth. In contrast, the combination treatment caused the regression of 3213-K and 1245-K tumors (**Fig. 5A** and **B**). The histologic analysis showed that MRTX1133 decreased pERK and induced BIM expression (Supplementary Figs. S5C and S9). Treatment with MRTX1133, either alone or in combination with venetoclax, decreased proliferation in all three KPC-K tumors (Supplementary Figs. S5C and S9). Whereas single-agent treatment with venetoclax induced apoptosis in the 1245-K tumors (Supplementary Fig. S9), the combination of MRTX1133 and venetoclax induced apoptosis in all three KPC-K tumors (Supplementary Figs. S5C and S9).

Discussion

There is increasing excitement with inhibitors targeting the RAS protein, which was previously considered undruggable (11, 12). The $KRAS^{G12C}$ inhibitors have received accelerated approval for lung cancer and are being considered for additional approvals as part of combination regimens (38). For example, the combination of the $KRAS^{G12C}$ inhibitor adagrasib and the EGFR antibody cetuximab is under FDA consideration as a subsequent-line treatment for colon cancers with the $KRAS^{G12C}$ mutation (39, 40). The $KRAS^{G12C}$ inhibitors have also been evaluated in pancreatic cancer, in which the $KRAS^{G12C}$ mutation is seen in only 1% to 2% of patients with pancreatic cancer (8). Clinical trials of inhibitors targeting $KRAS^{G12D}$, present in 40% to 45% of human PDAC tumors (6, 7), have recently been initiated (10–12). Given that the $KRAS^{G12C}$ inhibitors demonstrate a response rate of ~20% and a progression-free survival of ~4 to 5 months in pancreatic cancer (8, 9), it is likely that MRTX1133 and other $KRAS^{G12D}$ inhibitors will need to be combined with other drugs for enhanced antitumor response.

In this study, we show that venetoclax can enhance the efficacy of MRTX1133 in collagen cultures and in animal studies. Notably, we show that although MRTX1133 is effective in "low"-confluent collagen cultures, MRTX1133 has minimal to no effect when tested in "high"-confluent collagen cultures. Similarly, we show that whereas MRTX1133 has some activity in cells grown in low density on 2D tissue culture plastic, MRTX1133 has minimal activity when the cells are plated at high density. By BrdU staining, we show reduced proliferation under "high"-confluent collagen culture conditions compared with when cells are grown in "low"-confluent culture conditions, thus explaining the lack of response to single-agent treatment in "high"-confluent collagen culture conditions. Others have demonstrated that targeting KRAS is more effective in 3D than 2D cultures (34, 41, 42). Although our data agree with these previous observations when the cells are plated in low density in 2D and "low"-confluent collagen cultures in 3D, we show that the confluency of the cells in the 3D culture conditions can significantly limit the efficacy of MRTX1133. Nonetheless, our confluent collagen cultures enabled us to identify the combination regimen of venetoclax and MRTX1133 that shows efficacy *in vivo*.

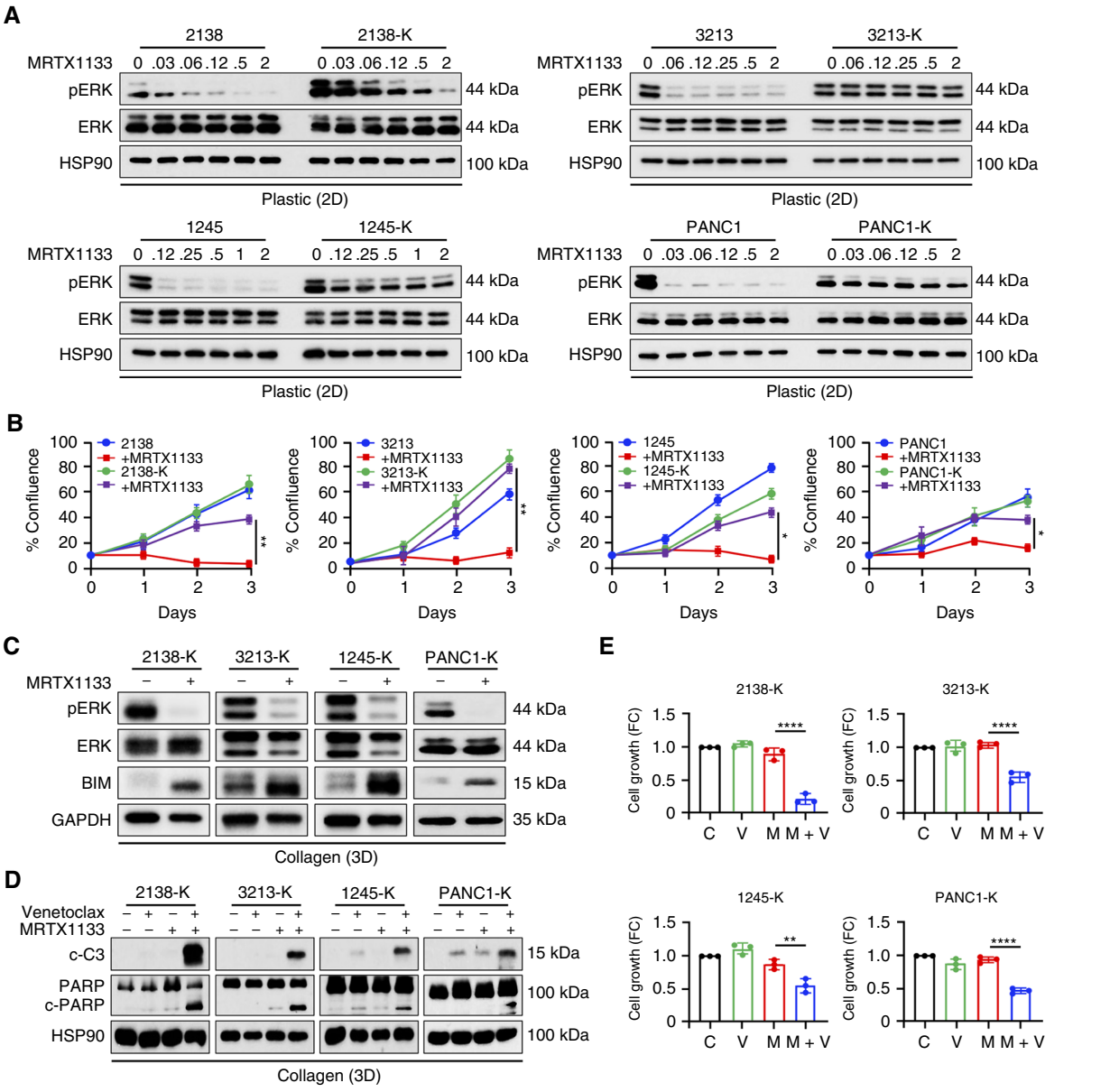

Figure 4.

MRTX1133-resistant cells respond to the combination of MRTX1133 and venetoclax in collagen cultures. PDAC (2138, 3213, 1245, and PANC1) cells were treated over 6 to 8 weeks with increasing concentrations of MRTX1133 to 2 μmol/L or greater to generate PDAC-K cells. **A,** PDAC and PDAC-K cells growing on tissue culture plastic were treated with increasing concentrations of MRTX1133 for 8 hours, and ERK activation was evaluated by Western blotting. Blots are representative of three biological replicates. **B,** PDAC and PDAC-K cells grown in "low"-confluent collagen cultures were treated with DMSO or 2 μmol/L MRTX1133 for 72 hours. The cells were imaged at baseline and after 1, 2, and 3 days of treatment, the relative growth was quantified. Error bars, ± SD, $n = 3$. Unpaired t test. **C,** PDAC-K cells growing in "high"-confluent collagen cultures were treated with MRTX1133 (2 μmol/L), and the effect on pERK and BIM protein levels was analyzed by Western blotting. Blots are representative of three biological replicates. **D,** PDAC-K cells in "high"-confluent collagen cultures were treated with venetoclax (2.5 μmol/L) and MRTX1133 (2.0 μmol/L) for 8 hours, and the effect on cell death (c-C3 and cleaved-PARP) was analyzed. Blots are representative of at least three biological replicates. **E,** PDAC-K cells growing in "high"-confluent collagen cultures were cotreated with venetoclax (V; 2.5 μmol/L) and MRTX1133 (M; 2.0 μmol/L) for 48 hours, and the effect on cell growth was analyzed. Error bars, ± SD, $n = 3$. One-way ANOVA, followed by the Tukey multiple comparison test. *, $P < 0.05$; **, $P < 0.01$; ****, $P < 0.0001$.

We show that the efficacy of the combination therapy is dependent on the increased MRTX1133-mediated BIM expression. Others have demonstrated that BIM is critical in mediating the response of inhibitors targeting the EGFR/RAS/RAF/MEK signaling pathway. Apoptosis induced by MEK inhibition in lung cancer cells is mediated by BIM (43). Similarly, EGFR inhibitor-induced apoptosis of lung cancer cells requires BIM, which is induced because of the suppression of MEK/ERK signaling (44). Moreover, the antitumor response of B-RAF mutant human tumor cells to MEK inhibition requires BIM (45). Similarly, induction of BIM expression

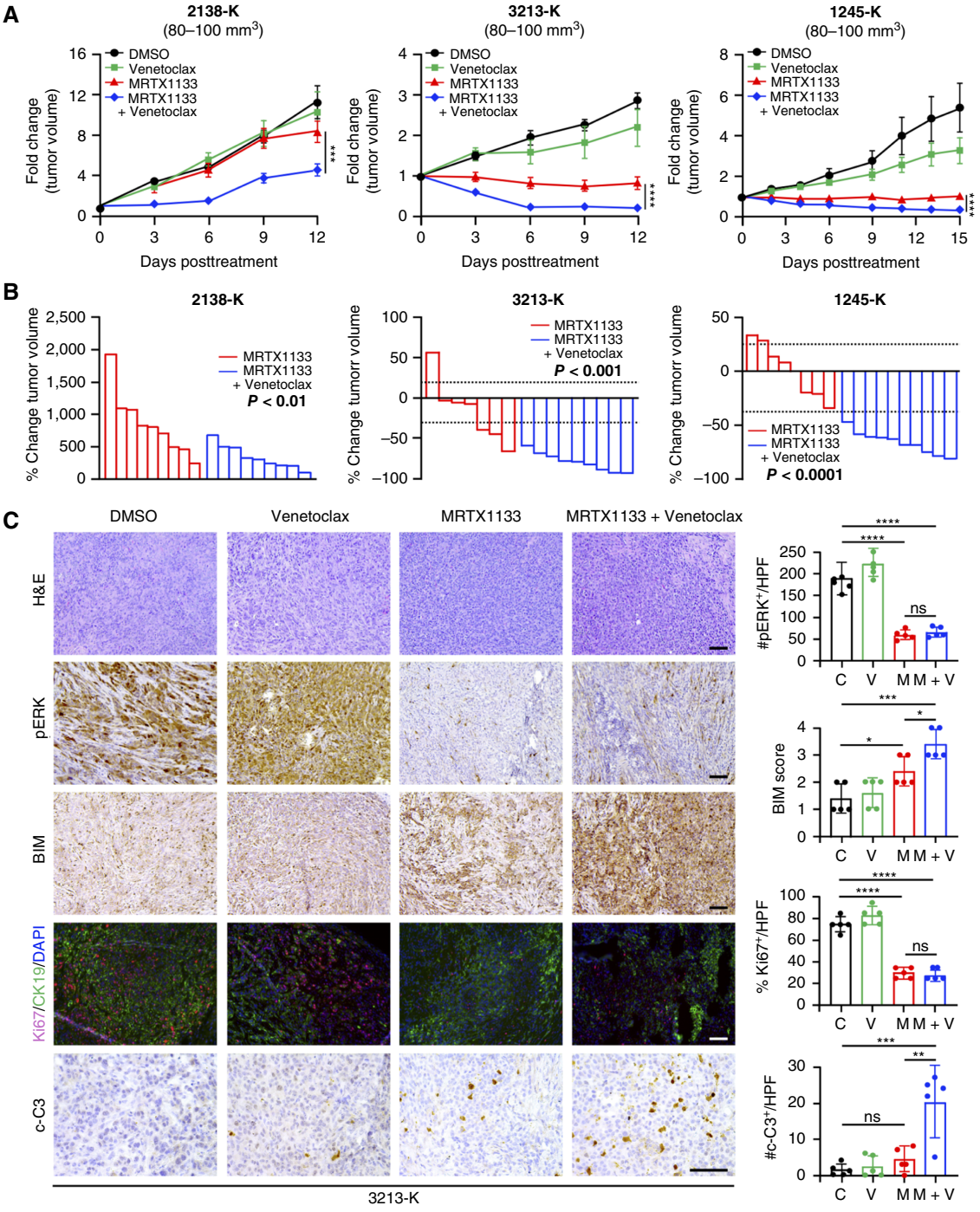

Figure 5.

Tumors established from KPC-K cells respond to the combination of MRTX1133 and venetoclax. The 2138-K, 3213-K, and 1245-K KPC cells (2.5×10^4) were implanted via subcutaneous injection into the flanks of C57BL/6 mice. Once animals developed ~80 to 100 mm^3 tumors, they were treated with vehicle control (DMSO), venetoclax (15 mg/kg daily), MRTX1133 (30 mg/kg 2×/day), or the combination of venetoclax and MRTX1133. **A,** Tumor size was measured 2 to 3 times/week by caliper, and tumor volume was calculated using the formula $V = (W^2 \times L)/2$ and normalized to tumor volume at the start of treatment. Error bars, ± SEM, $n = 7$–9 per treatment group. Significance between the MRTX1133-treated group and the combination treatment group was determined by two-way ANOVA with the Sidak multiple comparisons test. Changes in tumor volume between the dotted lines (−30%, +20%) were considered as stable disease. **B,** Relative tumor volumes at study endpoints were compared with tumors at the start of treatment, and change in tumor volume was calculated. Unpaired *t* test. **C,** 3213-K tumors at the study endpoints were hematoxylin and eosin (H&E)–stained and stained for pERK, BIM, the proliferation marker Ki67, the epithelial marker CK19, and the apoptosis marker c-C3. Error bars, ± SD. One-way ANOVA, followed by the Tukey multiple comparison test. *, $P < 0.05$; **, $P < 0.01$; ***, $P < 0.001$; ****, $P < 0.0001$; ns, not significant. Scale bars, 100 μm. C, DMSO; V, venetoclax; M, MRTX1133.

contributes to the response of the combination of sorafenib and a MEK inhibitor in hepatocellular carcinoma cells (46).

Although MRTX1133 increases BIM protein levels, we show that the increased BIM protein expression is not sufficient to induce apoptosis following single-agent treatment with MRTX1133 in "high"-confluent collagen cultures. This is consistent with reports in lung and pancreatic cancer models, in which the efficacy of MEK inhibitors can be increased by cotargeting the BCL2 family proteins (47). Similarly, the response of MEK inhibitors in B-RAF mutant human tumor cells and RAS/MAPK-mutated neuroblastoma cells can be enhanced by cotargeting the BCL2 family of proteins (45, 48). The combination of a MEK inhibitor and an inhibitor targeting the BCL2 family protein BCL-xL showed *in vivo* tumor regression in KRAS-mutant lung cancer models (49). Also, EGFR inhibitor-induced killing of lung cancer cells can be enhanced by cotargeting the BCL2 family proteins (44). We show that cotreatment with the BCL2 inhibitor venetoclax is required to induce apoptosis in "high"-confluent collagen cultures and *in vivo*.

We show that tumors established from parental KPC cell lines exhibit further regression when cotreated with MRTX1133 and venetoclax. Notably, a recent report showed that cancer cell killing and tumor regression in an immunocompetent model require $CD8^+$ T cells to induce apoptosis of cancer cells (15). Interestingly, MRTX1133 induces the expression of FAS on cancer cells, leading to the engagement of FAS ligand on $CD8^+$ T cells and subsequent killing of cancer cells through the extrinsic apoptotic pathway (15). Using our collagen culture model, we show that we need both BIM induction and BCL2 targeting to enhance apoptosis through the intrinsic apoptotic pathway with the combination regimen of venetoclax and MRTX1133.

We show that the combination therapy is also effective against cells that have become resistant to MRTX1133. Although these cells exhibit a reduced response to MRTX1133 suppression of pERK in 2D, we show that in 3D collagen cultures, MRTX1133 decreases pERK and increases BIM protein levels. The combination therapy suppresses growth and induces apoptosis in 3D collagen cultures. The combination therapy also causes tumor regression in two of the three resistant cell lines (3213-K and 1245-K). However, in the 2138-K tumors that grow rapidly *in vivo*, we show that although single-agent treatment with MRTX1133 does not affect their growth, the combination treatment significantly slows their growth. In future studies, we will evaluate whether replacing venetoclax with navitoclax, which targets BCL2, BCL-xL, and BCL-W (17, 50), in the combination treatment with MRTX1133 causes regression of 2138-K tumors *in vivo*.

In conclusion, our study underscores the potential of the combination of MRTX1133 and the FDA-approved drug venetoclax in promoting cell death and tumor regression, even in pancreatic tumors established from cells resistant to MRTX1133. Notably, there is increasing realization that venetoclax and other inhibitors targeting the BCL2 family proteins can overcome adaptive resistance to various therapies (18). Our results suggest testing venetoclax with MRTX1133 and other $KRAS^{G12D}$ inhibitors in patients with pancreatic cancer.

Authors' Disclosures

No disclosures were reported.

Disclaimer

The contents of this article are the responsibility of the authors and do not represent the views of the Department of Veterans Affairs or the US Government.

Authors' Contributions

J.H. Becker: Conceptualization, data curation, formal analysis, investigation, methodology, writing–original draft, writing–review and editing. **A.E. Metropulos:** Conceptualization, data curation, formal analysis, investigation, methodology, writing–original draft, writing–review and editing. **C. Spaulding:** Investigation, methodology, writing–review and editing. **A.M. Marinelarena:** Investigation, methodology, writing–review and editing. **M.A. Shields:** Investigation, methodology, writing–review and editing. **D.R. Principe:** Conceptualization, investigation, methodology, writing–review and editing. **T.D. Pham:** Conceptualization, data curation, formal analysis, investigation, methodology, writing–review and editing. **H.G. Munshi:** Conceptualization, data curation, supervision, funding acquisition, investigation, writing–original draft, writing–review and editing.

Acknowledgments

This work was supported by the Robert and Lora Lurie Endowed Professorship (to H.G. Munshi), the Harold E. Eisenberg Foundation (to H.G. Munshi), the Institutional Research Grant IRG-21-144-270 from the American Cancer Society (to T.D. Pham), the NIH/NCI training grant T32CA268935 (to A.M. Marinelarena), the NIH/NCI grant R01CA265997 (to H.G. Munshi), and the Department of Veterans Affairs grant I01BX005595 (to. H.G. Munshi). Parts of this work were performed at the Robert H. Lurie Comprehensive Cancer Center Pathology Core at Northwestern University, which is supported by the NCI CCSG P30 CA060553 awarded to the Robert H. Lurie Comprehensive Cancer Center.

Note

Supplementary data for this article are available at Cancer Research Online (http://cancerres.aacrjournals.org/).

Received November 13, 2023; revised May 22, 2024; accepted August 8, 2024; published first August 13, 2024.

References

1. Nevala-Plagemann C, Hidalgo M, Garrido-Laguna I. From state-of-the-art treatments to novel therapies for advanced-stage pancreatic cancer. Nat Rev Clin Oncol 2020;17:108–23.
2. Siegel RL, Giaquinto AN, Jemal A. Cancer statistics, 2024. CA Cancer J Clin 2024;74:12–49.
3. Principe DR, Kamath SD, Korc M, Munshi HG. The immune modifying effects of chemotherapy and advances in chemo-immunotherapy. Pharmacol Ther 2022;236:108111.
4. Collins MA, Bednar F, Zhang Y, Brisset J-C, Galbán S, Galbán CJ, et al. Oncogenic Kras is required for both the initiation and maintenance of pancreatic cancer in mice. J Clin Invest 2012;122:639–53.
5. Simanshu DK, Nissley DV, McCormick F. RAS proteins and their regulators in human disease. Cell 2017;170:17–33.
6. Hofmann MH, Gerlach D, Misale S, Petronczki M, Kraut N. Expanding the reach of precision oncology by drugging all KRAS mutants. Cancer Discov 2022;12:924–37.
7. Prior IA, Hood FE, Hartley JL. The frequency of ras mutations in cancer. Cancer Res 2020;80:2969–74.
8. Strickler JH, Satake H, George TJ, Yaeger R, Hollebecque A, Garrido-Laguna I, et al. Sotorasib in KRAS p.G12C-mutated advanced pancreatic cancer. N Engl J Med 2023;388:33–43.
9. Bekaii-Saab TS, Yaeger R, Spira AI, Pelster MS, Sabari JK, Hafez N, et al. Adagrasib in advanced solid tumors harboring a $KRAS^{G12C}$ mutation. J Clin Oncol 2023;41:4097–106.
10. Wei D, Wang L, Zuo X, Maitra A, Bresalier RS. A small molecule with big impact: MRTX1133 targets the KRASG12D mutation in pancreatic cancer. Clin Cancer Res 2024;30:655–62.

11. Singhal A, Li BT, O'Reilly EM. Targeting KRAS in cancer. Nat Med 2024;30:969–83.
12. Perurena N, Situ L, Cichowski K. Combinatorial strategies to target RAS-driven cancers. Nat Rev Cancer 2024;24:316–37.
13. Hallin J, Bowcut V, Calinisan A, Briere DM, Hargis L, Engstrom LD, et al. Anti-tumor efficacy of a potent and selective non-covalent $KRAS^{G12D}$ inhibitor. Nat Med 2022;28:2171–82.
14. Kemp SB, Cheng N, Markosyan N, Sor R, Kim I-K, Hallin J, et al. Efficacy of a small-molecule inhibitor of KrasG12D in immunocompetent models of pancreatic cancer. Cancer Discov 2023;13:298–311.
15. Mahadevan KK, McAndrews KM, LeBleu VS, Yang S, Lyu H, Li B, et al. $KRAS^{G12D}$ inhibition reprograms the microenvironment of early and advanced pancreatic cancer to promote FAS-mediated killing by $CD8^+$ T cells. Cancer Cell 2023;41:1606–20.e8.
16. Youle RJ, Strasser A. The BCL-2 protein family: opposing activities that mediate cell death. Nat Rev Mol Cell Biol 2008;9:47–59.
17. Ploumaki I, Triantafyllou E, Koumprentziotis I-A, Karampinos K, Drougkas K, Karavolias I, et al. Bcl-2 pathway inhibition in solid tumors: a review of clinical trials. Clin Transl Oncol 2023;25:1554–78.
18. Montero J, Haq R. Adapted to survive: targeting cancer cells with BH3 mimetics. Cancer Discov 2022;12:1217–32.
19. Luciano F, Jacquel A, Colosetti P, Herrant M, Cagnol S, Pages G, et al. Phosphorylation of Bim-EL by Erk1/2 on serine 69 promotes its degradation via the proteasome pathway and regulates its proapoptotic function. Oncogene 2003;22:6785–93.
20. Ley R, Balmanno K, Hadfield K, Weston C, Cook SJ. Activation of the ERK1/2 signaling pathway promotes phosphorylation and proteasome-dependent degradation of the BH3-only protein, Bim. J Biol Chem 2003;278:18811–6.
21. Iavarone C, Zervantonakis IK, Selfors LM, Palakurthi S, Liu JF, Drapkin R, et al. Combined MEK and BCL-2/X_L inhibition is effective in high-grade serous ovarian cancer patient-derived xenograft models and BIM levels are predictive of responsiveness. Mol Cancer Ther 2019;18:642–55.
22. Shields MA, Spaulding C, Metropulos AE, Khalafalla MG, Pham TND, Munshi HG. Gα13 loss in Kras/Tp53 mouse model of pancreatic tumorigenesis promotes tumors susceptible to rapamycin. Cell Rep 2022;38:110441.
23. Nielsen SR, Quaranta V, Linford A, Emeagi P, Rainer C, Santos A, et al. Macrophage-secreted granulin supports pancreatic cancer metastasis by inducing liver fibrosis. Nat Cell Biol 2016;18:549–60.
24. Munshi HG, Stack MS. Analysis of matrix degradation. Methods Cell Biol 2002;69:195–205.
25. Randriamanantsoa S, Papargyriou A, Maurer HC, Peschke K, Schuster M, Zecchin G, et al. Spatiotemporal dynamics of self-organized branching in pancreas-derived organoids. Nat Commun 2022;13:5219.
26. Linnemann JR, Miura H, Meixner LK, Irmler M, Kloos UJ, Hirschi B, et al. Quantification of regenerative potential in primary human mammary epithelial cells. Development 2015;142:3239–51.
27. Pham TN, Spaulding C, Shields MA, Metropulos AE, Shah DN, Khalafalla MG, et al. Inhibition of MNKs promotes macrophage immunosuppressive phenotype to limit $CD8^+$ T cell antitumor immunity. JCI Insight 2022;7:e152731.
28. Principe DR, Aissa AF, Kumar S, Pham TND, Underwood PW, Nair R, et al. Calcium channel blockers potentiate gemcitabine chemotherapy in pancreatic cancer. Proc Natl Acad Sci U S A 2022;119:e2200143119.
29. Sahai V, Kumar K, Knab LM, Chow CR, Raza SS, Bentrem DJ, et al. BET bromodomain inhibitors block growth of pancreatic cancer cells in three-dimensional collagen. Mol Cancer Ther 2014;13:1907–17.
30. Senkevitch E, Li W, Hixon JA, Andrews C, Cramer SD, Pauly GT, et al. Inhibiting Janus Kinase 1 and BCL-2 to treat T cell acute lymphoblastic leukemia with IL7-Rα mutations. Oncotarget 2018;9:22605–17.
31. Pham TND, Kumar K, DeCant BT, Shang M, Munshi SZ, Matsangou M, et al. Induction of MNK kinase-dependent eIF4E phosphorylation by inhibitors targeting BET proteins limits efficacy of BET inhibitors. Mol Cancer Ther 2019;18:235–44.
32. Bardeesy N, DePinho RA. Pancreatic cancer biology and genetics. Nat Rev Cancer 2002;2:897–909.
33. Shields MA, Dangi-Garimella S, Redig AJ, Munshi HG. Biochemical role of the collagen-rich tumour microenvironment in pancreatic cancer progression. Biochem J 2012;441:541–52.
34. Kumarasamy V, Wang J, Frangou C, Wan Y, Dynka A, Rosenheck H, et al. The extracellular niche and tumor microenvironment enhance KRAS inhibitor efficacy in pancreatic cancer. Cancer Res 2024;84:1115–32.
35. Waters AM, Der CJ. KRAS: the critical driver and therapeutic target for pancreatic cancer. Cold Spring Harb Perspect Med 2018;8:a031435.
36. Souers AJ, Leverson JD, Boghaert ER, Ackler SL, Catron ND, Chen J, et al. ABT-199, a potent and selective BCL-2 inhibitor, achieves antitumor activity while sparing platelets. Nat Med 2013;19:202–8.
37. Hari Y, Harashima N, Tajima Y, Harada M. Bcl-xL inhibition by molecular-targeting drugs sensitizes human pancreatic cancer cells to TRAIL. Oncotarget 2015;6:41902–15.
38. Torres-Jimenez J, Espinar JB, de Cabo HB, Berjaga MZ, Esteban-Villarrubia J, Fraile JZ, et al. Targeting $KRAS^{G12C}$ in non-small-cell lung cancer: current standards and developments. Drugs 2024;84:527–48.
39. Yaeger R, Uboha NV, Pelster MS, Bekaii-Saab TS, Barve M, Saltzman J, et al. Efficacy and safety of adagrasib plus cetuximab in patients with KRASG12C-mutated metastatic colorectal cancer. Cancer Discov 2024;14:982–93.
40. Yaeger R, Weiss J, Pelster MS, Spira AI, Barve M, Ou S-HI, et al. Adagrasib with or without cetuximab in colorectal cancer with mutated KRAS G12C. N Engl J Med 2023;388:44–54.
41. Janes MR, Zhang J, Li L-S, Hansen R, Peters U, Guo X, et al. Targeting KRAS mutant cancers with a covalent G12C-specific inhibitor. Cell 2018;172:578–89.e17.
42. Muzumdar MD, Chen P-Y, Dorans KJ, Chung KM, Bhutkar A, Hong E, et al. Survival of pancreatic cancer cells lacking KRAS function. Nat Commun 2017;8:1090.
43. Meng J, Fang B, Liao Y, Chresta CM, Smith PD, Roth JA. Apoptosis induction by MEK inhibition in human lung cancer cells is mediated by Bim. PLoS One 2010;5:e13026.
44. Cragg MS, Kuroda J, Puthalakath H, Huang DCS, Strasser A. Gefitinib-induced killing of NSCLC cell lines expressing mutant EGFR requires BIM and can be enhanced by BH3 mimetics. PLoS Med 2007;4:1681–9.
45. Cragg MS, Jansen ES, Cook M, Harris C, Strasser A, Scott CL. Treatment of B-RAF mutant human tumor cells with a MEK inhibitor requires Bim and is enhanced by a BH3 mimetic. J Clin Invest 2008;118:3651–9.
46. Ou D-L, Shen Y-C, Liang J-D, Liou J-Y, Yu S-L, Fan H-H, et al. Induction of Bim expression contributes to the antitumor synergy between sorafenib and mitogen-activated protein kinase/extracellular signal-regulated kinase kinase inhibitor CI-1040 in hepatocellular carcinoma. Clin Cancer Res 2009;15:5820–8.
47. Tan N, Wong M, Nannini MA, Hong R, Lee LB, Price S, et al. Bcl-2/Bcl-xL inhibition increases the efficacy of MEK inhibition alone and in combination with PI3 kinase inhibition in lung and pancreatic tumor models. Mol Cancer Ther 2013;12:853–64.
48. Eleveld TF, Vernooij L, Schild L, Koopmans B, Alles LK, Ebus ME, et al. MEK inhibition causes BIM stabilization and increased sensitivity to BCL-2 family member inhibitors in RAS-MAPK-mutated neuroblastoma. Front Oncol 2023;13:1130034.
49. Corcoran RB, Cheng KA, Hata AN, Faber AC, Ebi H, Coffee EM, et al. Synthetic lethal interaction of combined BCL-XL and MEK inhibition promotes tumor regressions in KRAS mutant cancer models. Cancer Cell 2013;23:121–8.
50. Tse C, Shoemaker AR, Adickes J, Anderson MG, Chen J, Jin S, et al. ABT-263: a potent and orally bioavailable Bcl-2 family inhibitor. Cancer Res 2008;68:3421–8.